Quantum Electronics **41** (4) 387 – 392 (2011)

LASER NANOTECHNOLOGIES

PACS numbers: 81.16.–c; 78.67.–n; 42.65.Re
DOI: 10.1070/QE2011v041n04ABEH014464

Surface nanostructuring of Ni/Cu foils by femtosecond laser pulses

V.P. Korolkov, A.A. Ionin, S.I. Kudryashov, L.V. Seleznev, D.V. Sinitsyn, R.V. Samsonov, A.I. Masliy, A.Zh. Medvedev, B.G. Goldenberg

***Abstract*. This work examines the effect of high-power femtosecond laser pulses on Ni/Cu bilayer foils produced by electrodeposition. We consider nanostructures formed at different laser beam parameters and under different ambient conditions. The surface nanostructures obtained in air and water have mostly the form of quasi-periodic ripples with a characteristic period of 400 – 450 and 370 – 390 nm, respectively, at a laser wavelength of 744 nm, whereas the nanostructures produced in ethanol and benzine have the form of spikes, typically spaced 400 – 700 nm apart. Femtosecond laser nanostructuring of metals is for the first time proposed, and experimentally tested, as a viable approach to producing anti-reflective coatings on the surface of polymer replicas.**

Keywords: *femtosecond laser nanostructuring, anti-reflective coatings, diffractive optics.*

1. Introduction

Recent work has shown that high-power femtosecond laser pulses incident on the surface of some metals (tantalum, nickel, copper, tungsten and others) and semiconductors (silicon and germanium) produce quasi-periodic surface nanostructures with a characteristic period, 100 – 800 nm, smaller than the laser wavelength [1 – 10]. According to a number of hypotheses [1, 2, 9, 11], the formation of such structures can be accounted for in terms of a universal polariton ('interference') model [3, 12, 13] and is due to the interference between the incident electromagnetic wave and the surface plasmons it excites, as evidenced by the particular character of ablation near individual nanodefects and by the fact that rapid ablation occurs only locally. Makin et al. [3] think that laser pulses incident on a material in air generate a nonequilibrium plasma on its surface, resulting in local surface oxidation. This influences the wavelength of the excited surface electromagnetic wave and, hence, the period of the forming surface profile [12, 13].

The structures (gratings) in question may impart unique, wavelength-dependent physical and chemical properties to the surface [5] and may act as nanoparticle sources [1, 2, 5 – 7]. A noteworthy feature of nanostructured surfaces is their ability to absorb almost all the visible and near-IR light incident on them. In particular, this effect can be employed to produce anti-reflective coatings of high-efficiency photodetectors and emitters for converting the combustion energy spectrum to the spectral range where photoelectric detectors have the highest sensitivity. The ability to transfer such a surface relief nanopattern from a metal to the surface of transparent materials via a replication process would allow one to envisage a novel, promising application area for femtosecond laser nanostructuring (FLN): fabrication of anti-reflective non-absorbing coatings for optical elements.

Coatings of this type are produced as subwavelength grating structures. Such gratings exhibit only zero-order diffraction and change the effective refractive index in the surface layer of the material. At the same time, the anti-reflective properties of linear subwavelength gratings depend on the incident wave polarisation. Subwavelength gratings are commonly fabricated by interference lithography using a photoresist layer and short-wavelength laser sources. This approach is however only applicable to flat surfaces. Nikolajeff et al. [14] experimentally demonstrated the feasibility of writing a subwavelength grating coating by an electron beam and simultaneously forming the topology of the diffractive optical element, but the method proved very time-consuming and expensive.

The replication of optical elements through thermo- and photopolymerisation and injection moulding (in particular, using glass) is widely employed to mass produce diffractive optics, microoptics and aspherical lenses. Eliminating the classic anti-reflective coating deposition step by creating a nanostructured injection mould might significantly simplify the optical element fabrication process. This is of particular interest for diffractive optical elements because a classic sputter-deposited coating smooths out the diffraction microrelief profile, thereby considerably reducing the diffraction efficiency.

V.P. Korolkov Institute of Automation and Electrometry, Siberian Branch, Russian Academy of Sciences, prosp. Akad. Koptyuga 1, 630090 Novosibirsk, Russia; e-mail: vkorolkov@yandex.ru;
A.A. Ionin, S.I. Kudryashov, L.V. Seleznev, D.V. Sinitsyn P.N. Lebedev Physics Institute, Russian Academy of Sciences, Leninsky prosp. 53, 119991 Moscow, Russia; e-mail: sikudr@sci.lebedev.ru;
R.V. Samsonov Novosibirsk State University, ul. Pirogova 2, 630090 Novosibirsk, Russia;
A.I. Masliy, A.Zh. Medvedev Institute of Solid-State Chemistry and Mechanochemistry, Siberian Branch, Russian Academy of Sciences, ul. Kutateladze 18, 630128 Novosibirsk, Russia;
B.G. Goldenberg G.I. Budker Institute of Nuclear Physics, Siberian Branch, Russian Academy of Sciences, prosp. Akad. Lavrent'eva 11, 630090 Novosibirsk, Russia

Received 20 October 2010; revision received 17 December 2010
Kvantovaya Elektronika **41** (4) 387 – 392 (2011)
Translated O.M. Tsarev

Nickel is a typical material for the electroforming replication of diffractive optical structures and microoptics. This work is the first to examine the FLN of electrodeposited nanocrystalline nickel films and to demonstrate the possibility of replicating the nanostructure on the surface of optically transparent polymers. We also analyse the optical properties of the surface-nanostructured polymer replicas in order to verify whether such coatings have antireflective properties.

2. FLN experiments with nickel foils

First, we studied the effect of multiple weakly focused high-power femtosecond Ti : sapphire laser pulses (centre wavelength, 744 nm; pulse duration, 110 fs; pulse energy, up to 5 mJ; beam spot diameter, ~ 1 mm; pulse repetition rate, 10 Hz) on Ni/Cu bilayer foils at a scan rate of 6 μm s^{-1}. The foils were prepared as follows: First, an optically polished glass substrate carrying a chemically deposited thin silver layer was coated with a 30- to 50-μm-thick low-stress copper layer, which was deposited from a binary sulphate electrolyte solution containing bis(sodium sulphopropyl) disulphide additions. The flat copper replica was then separated from the glass substrate (together with the silver underlayer) and a 3- to 10-μm-thick functional nanocrystalline nickel layer was electrodeposited onto its frontside [15]. The thick copper layer ensured sufficient rigidity and planarity of the Ni/Cu foil and improved heat removal during laser processing.

The use of nanocrystalline nickel was critical for our purposes because previous studies concerned with the FLN of metals had employed polished specimens of cast, coarse-grained metals. We assumed that the previously observed erosion of laser-written linear gratings (see e.g. Golosov et al. [9]) had been initiated at grain boundaries and that the much smaller grain size in electrodeposited films would enable the fabrication of more ordered gratings.

We investigated nanostructures produced on specimen surfaces by linearly polarised laser radiation at an energy density of 50 – 300 mJ cm^{-2} in different media (air, distilled water, reagent-grade ethanol and benzine). FLN under a liquid layer was performed in order to assess the feasibility of producing two-dimensional (2D) nanostructures with polarisation-independent optical properties.

Surface topography was examined on a Carl Zeiss AxioImager optical microscope and Hitachi S3400N scanning electron microscope (SEM). The results demonstrate that exposure under certain conditions in air or through a thin (1 – 1.5 mm) water layer produces quasi-periodic surface trenches (ripple pattern) with a characteristic period of 400 – 450 (Fig. 1a) or 370 – 390 nm (Fig. 1b). As expected, the wave vector of the gratings thus formed is parallel to the polarisation direction of the laser beam (in accordance with polariton interference model predictions [3, 12, 13], rotating the specimen or the polarisation direction of the incident beam causes the resulting nanograting to rotate, as shown by Huang et al. [7], and the grating period is closely related to the laser wavelength [7, 8]). When the process is run in water, grating formation is to some extent obscured by the contamination of the film surface with nanoparticles, which may differ in chemical nature from the film in the case of nickel [16] (e.g., nickel oxide nanoparticles) and other target materials [17]. In the other liquids tested, no nanoparticles were formed, and we obtained nanospike arrays (Figs 1c, 1d) instead of surface nanoripples.

As an example, Fig. 2a shows the Fourier spectrum of

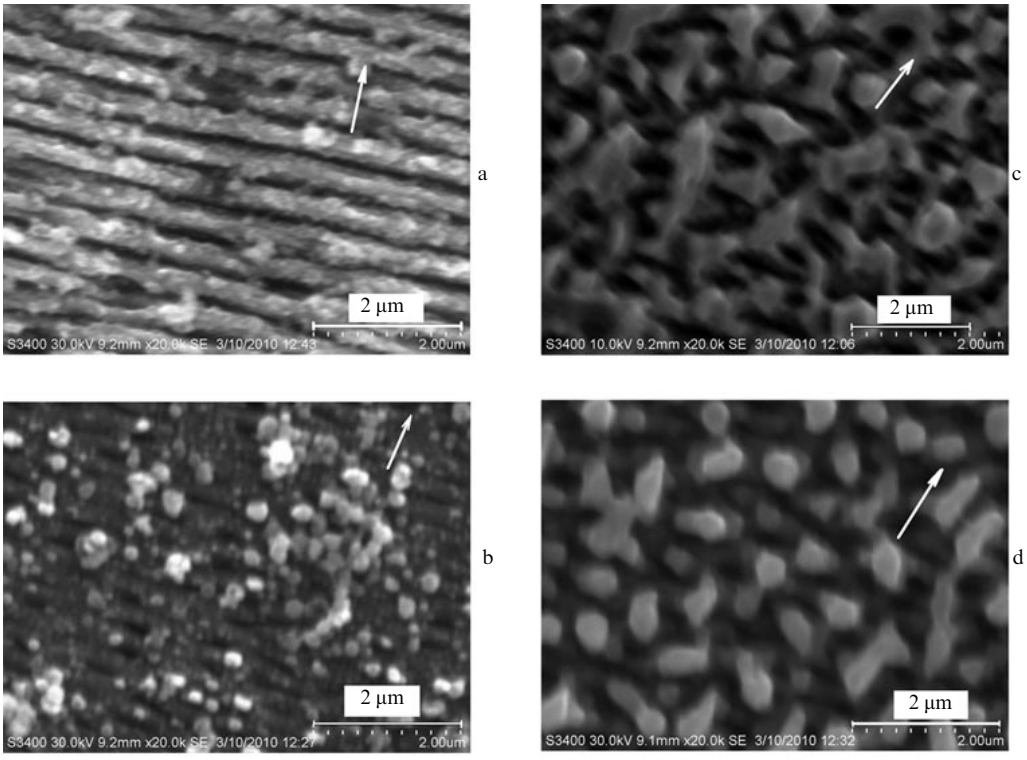

Figure 1. SEM images of nanostructures produced (a) in air at a laser fluence $F = 150$ mJ cm^{-2}, (b) in water at $F = 100$ mJ cm^{-2}, (c) in ethanol at $F = 100$ mJ cm^{-2} and (d) in benzine at $F = 90$ mJ cm^{-2}. The arrows indicate the polarisation direction of the laser beam.

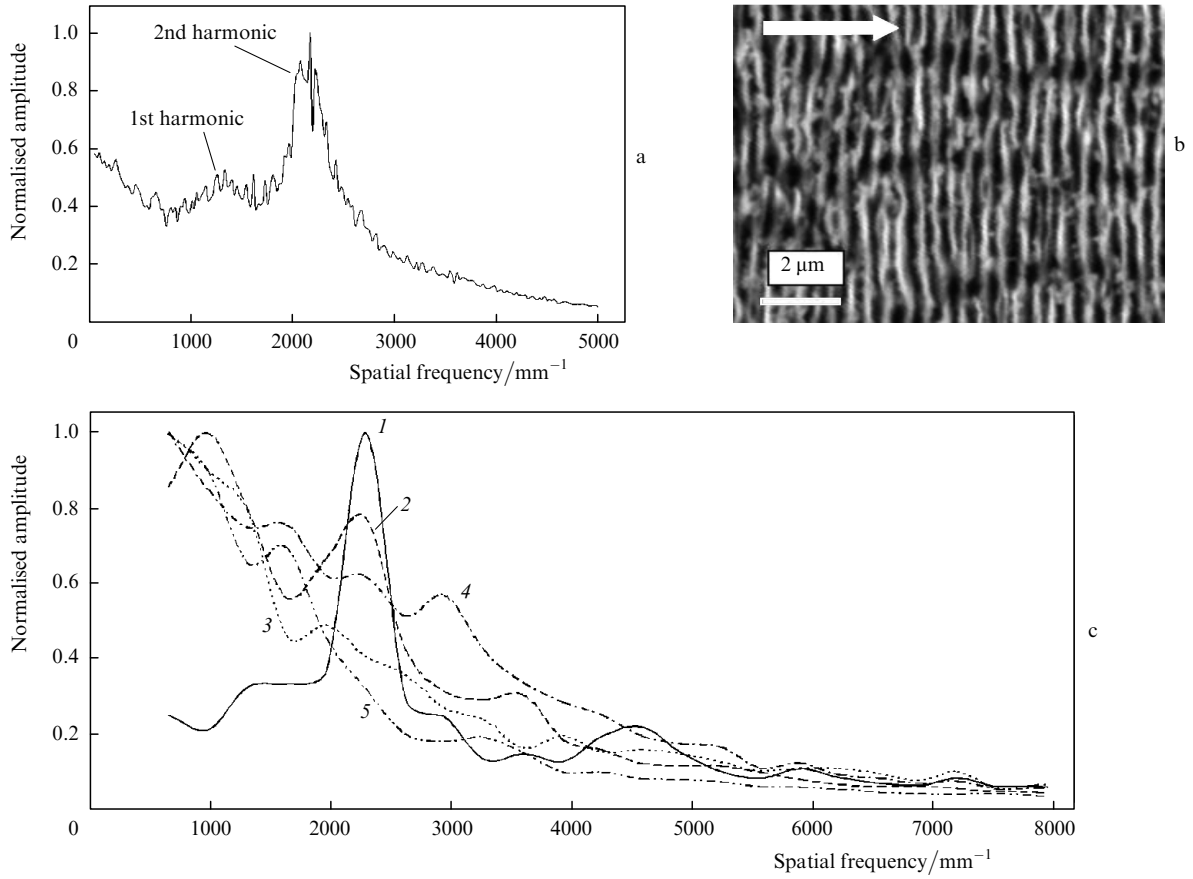

Figure 2. (a) Fourier spectrum of the SEM image in panel (b) (exposure in air at a laser fluence $F = 150$ mJ cm^{-2}). (c) Fourier spectra of SEM images of surface structures produced (*1*) in air at $F = 200$ mJ cm^{-2}; (*2*, *3*) in ethanol at $F = 100$ and 150 mJ cm^{-2}, respectively; (*4*) in water at $F = 100$ mJ cm^{-2} and (*5*) in benzine at $F = 90$ mJ cm^{-2}. The arrow indicates the polarisation direction of the laser beam.

the SEM image in Fig. 2b. The spectrum was obtained by calculating the Fourier spectrum of each horizontal scan line (along the polarisation direction) and averaging over all the lines. There is a prominent peak near a spatial frequency of 2200 mm^{-1}, which corresponds to a grating period of 450 nm. There is also a weaker, but distinct, peak at ~ 1330 mm^{-1}. The spatial period of such a structure (750 nm) differs very little from the wavelength of the femtosecond laser used. The positions of the peaks in the Fourier spectrum suggest that they roughly correspond to the first and second harmonics of the surface nanoripple pattern in Fig. 1a. It is remarkable that the second harmonic of surface ripples was also observed in earlier studies (e.g. on InP [18]), but its amplitude was always smaller than that of the fundamental (first) harmonic [18, 19]. This effect may be due to the nonsinusoidal profile of the intermediate nanoripple pattern (similar to that in Fig. 1a), which evolves under the effect of femtosecond laser pulses [20]. As a result, the angular spectrum of diffracted radiation is dominated by a field component [21] that interferes with the incident electromagnetic wave to generate the corresponding harmonic of the nanoripple pattern.

Figure 2c shows average Fourier spectra of surface nanostructures obtained under different exposure conditions (in different media). Like the spectrum in Fig. 2a, the Fourier spectra were calculated along the polarisation direction and averaged over all the image lines. Also shown for comparison is the spectrum of a surface structure produced in air, which has a prominent peak. It can be seen that there are surface features at spatial frequencies from 1500 to 3100 mm^{-1}, which roughly correspond to sizes from 700 to 300 nm. The fact that no ripple pattern was obtained in the liquids may be due to the complex character of light refraction in boiling liquids, the motion of the molten material and nanoripple degradation [22]. The characteristic size of the nanospikes produced on the foils by exposure in water is ~ 300 nm, in agreement with the peak at 3000 mm^{-1} in curve (*4*) in Fig. 2c. Because there are nanospikes less than 300 nm in size, curve (*4*) lies above the other curves at high spatial frequencies (up to 5500 mm^{-1}).

3. Replication of nanostructures and optical properties of the replicas

We also examined whether the FLN of metals could be used to produce an anti-reflective coating on polymer replicas of the surface relief pattern on a metal. A subwavelength surface grating with a period much smaller than the incident radiation wavelength behaves as a homogeneous medium with a refractive index smaller than that of the parent material. According to theoretical studies based on Rytov's fundamental work [23], the reflectance of a surface covered with subwavelength gratings can be substantially reduced in a wide spectral range and a wide range of angles of observation [24–26].

Since the period of subwavelength gratings that ensure anti-reflective properties of a dielectric surface should not

exceed half the incident radiation wavelength, with the characteristic nanostructure periods obtained in this study (400 – 450 nm) anti-reflective properties may show up in the near-IR spectral region. The surface profile depth of a polymer replica then should be at least 200 nm (Fig. 3) at a refractive index of the polymer in the range 1.5 – 1.6. It is also known that crossed gratings and 2D regular spikelike structures are preferable for producing less polarisation-sensitive anti-reflective coatings.

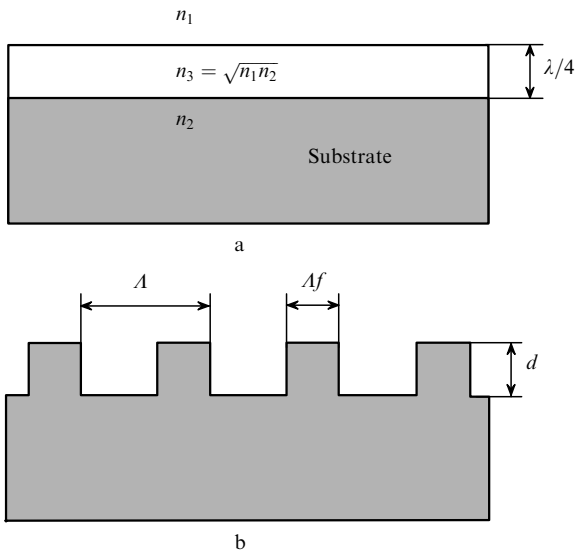

Figure 3. Geometric parameters of anti-reflective coatings based on (a) a thin film and (b) a subwavelength binary phase grating: n_1, n_2 and n_3 are the refractive indices of the medium, substrate and film, respectively; Λ and d are the grating period and depth; λ is the incident radiation wavelength; f is the grating duty cycle ($0 < f < 1$); and $d = \sqrt{n_1 n_2}\lambda/4$.

Our interest in the FLN of nickel stems from the assumption that it can be applied in the technology of diffractive optical elements with an anti-reflective surface nanostructure. The fabrication process may include the following steps (Fig. 4a): laser direct writing of a primary diffraction microrelief profile into photoresist (steps 1 and 2), fabrication of a nickel copy of the photoresist master by electroplating (steps 3 and 4), exposure of the nickel copy (stamper) to femtosecond laser pulses in order to write subwavelength nanogratings (steps 5 and 6) and replication of the hybrid profile on the surface of an optically transparent polymer by hot embossing or photopolymerisation (steps 7 and 8).

In our experiments, we used a simplified process for the fabrication of nanostructures on the surface of optically transparent polymer layers (Fig. 4b). Copper/nickel foil that was prepared as described above and had a mirror-smooth surface was exposed to femtosecond laser pulses in order to produce a nanoripple pattern (step 1). The pattern was then replicated on the surface of a transparent polymer (PMMA) by hot embossing or photopolymerisation of the hybrid photopolymer Ormocomp [27] (steps 2 and 3). Figure 5 shows an exposed Ni/Cu foil and its polymer replica.

Figure 6 presents transmission spectra of polymer replicas of unexposed and exposed areas of Ni/Cu foil (Shimadzu UV-3600 spectrophotometer). As seen, the coating strongly scatters near-IR and visible light. At the same time, at wavelengths above 1670 nm the surface nanostructure produced by replicating the foil exposed to a laser fluence of 200 mJ cm^{-2} begins to exhibit anti-reflective

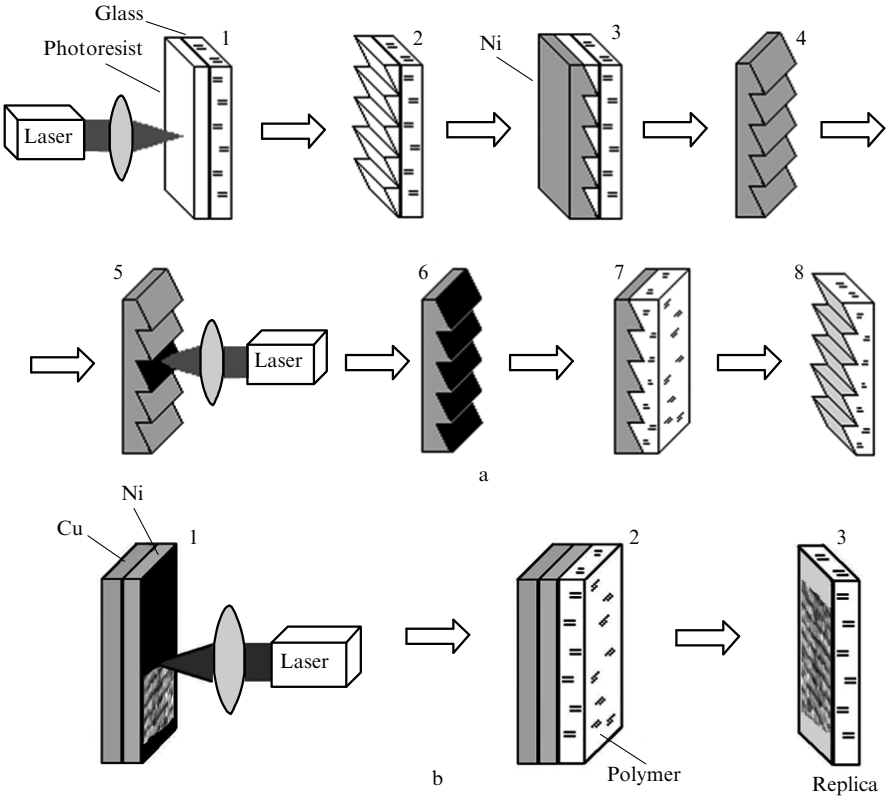

Figure 4. Schematics of (a) the proposed process for the fabrication of diffractive optical elements with an anti-reflective surface nanostructure and (b) the implemented process for the fabrication of nanostructured polymer replicas. The numbers specify the steps of the processes.

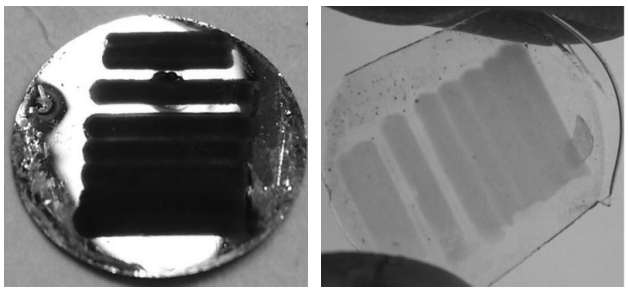

a b

Figure 5. (a) Ni/Cu foil nanostructured by femtosecond laser pulses in ethanol and (b) its transparent replica on the surface of the hybrid photopolymer Ormocomp.

properties. In the range 1700 – 2200 nm, the increase in transmittance is 3 % – 7 %. At wavelengths above ~ 2250 nm, the transmittance of the replica of the exposed area sharply rises by ~ 20 %. We cannot gain insight into the mechanism of this sharp rise in transmittance because the refractive index of Ormocomp at wavelengths above 1550 nm is not available in the literature.

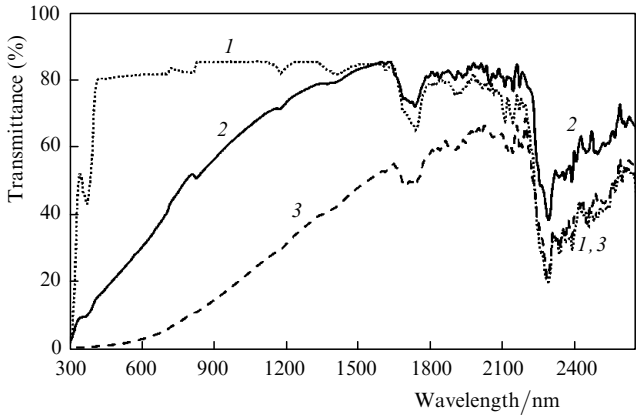

Figure 6. Transmission spectra of Ormocomp replicas of (*1*) unexposed and (*2, 3*) exposed areas of Ni/Cu foil: $F = 200$ (*2*) and 300 mJ cm^{-2} (*3*).

Figure 7 is an optical micrograph of Ni/Cu foil after exposure to femtosecond laser pulses. One can see structures with a characteristic length scale of the order of several microns. Incident light is diffracted by these structures, which leads to reflected light energy losses. Anti-reflective properties of the nanostructure were observed at longer wavelengths than was expected. The likely reason for this is that it had a more complex surface profile than the binary profile in Fig. 3b.

A necessary condition for the ability to produce diffractive optical elements with an anti-reflective surface nanostructure (Fig. 4a) is that the FLN of the stamper surface should not significantly distort the original diffraction microrelief profile. Our experimental data demonstrate that the surface layer removed through laser ablation in the FLN process was no thicker than 150 – 200 nm. This is quite acceptable in the fabrication of diffractive elements with a typical depth of 1 – 1.5 μm (Fig. 4a).

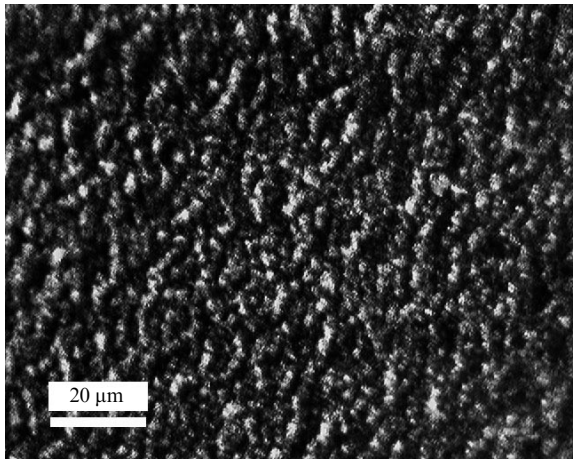

Figure 7. Optical micrograph of the surface of nanostructured Ni/Cu foil (Carl Zeiss AxioImager, exposure in air, $F = 150$ mJ cm^{-2}).

4. Conclusions

We have studied surface nanostructures generated on Ni/Cu foils by femtosecond laser pulses. The foils were produced by electrodeposition under conditions that ensured an essentially amorphous structure of the nickel front surface. The nanostructures generated on nickel by a laser beam in air and water had for the most part the form of ripples. On a smaller length scale, we observed erosion, directed largely along the ripples, like in the case of microcrystalline metals exposed to femtosecond laser pulses. Thus, there is conclusive evidence that the microstructure of the metal does not play a key role in determining nanoripple degradation. Increasing the laser fluence in the range 150 – 200 mJ cm^{-2} (in air) enables the fabrication of more ordered gratings. The wave vector of the gratings is parallel to the polarisation direction of the laser beam.

When the foils were exposed through an organic liquid (benzine or ethanol) layer, no ripples were formed, which can be interpreted in terms of erosion of the surface profile.

This work is the first to demonstrate the possibility of producing anti-reflective coatings on polymeric diffractive optical elements through the replication of the master profile formed on photoresist by photolithography or laser direct writing.

Acknowledgements. This work was supported in part by the Siberian Branch of the Russian Academy of Sciences (Interdisciplinary Project No. 55) and the Russian Foundation for Basic Research (Grant Nos 09-02-12018-ofi_m, 09-02-01065-a, 10-08-00941-a, 11-02-01202-a and 11-08-01165-a).

References

1. Zabotnov S.V., Golovan' L.A., Ostapenko I.A., et al. *Pis'ma Zh. Eksp. Teor. Fiz.*, **83**, 76 (2006).
2. Vorobyev A.Y., Makin V.S., Guo C. *J. Appl. Phys.*, **101**, 034903 (2007).
3. Makin V.S., Makin R.S., Vorobyev A.Ya., Guo C. *Pis'ma Zh. Tekh. Fiz.*, **34**, 55 (2008).
4. Wagner R., Gottmann J., Horn A., Kreutz E.W. *Appl. Surf. Sci.*, **252**, 8576 (2006).

5. Yang Y., Yang J., Liang C., Wang H. *Opt. Express*, **16**, 11259 (2008).
6. Miyaji G., Miyazaki K. *Opt. Express*, **16**, 16265 (2008).
7. Huang M., Zhao F., Cheng Y., et al. *Opt. Express*, **16**, 19354 (2008).
8. Huang M., Zhao F., Cheng Y., et al. *Phys. Rev. B*, **79**, 125436 (2009).
9. Golosov E.V., Ionin A.A., Kudryashov S.I., et al. *Pis'ma Zh. Eksp. Teor. Fiz.*, **90**, 116 (2009).
10. Liu X., Wang Y. *Chin. Opt. Lett.,* **3**, 1 (2005).
11. Sakabe S., Hashida M., Tokita S., et al. *Phys. Rev. B*, **79**, 033409 (2009).
12. Akhmanov S.A., Emel'yanov V.I., Koroteev N.I., Seminogov V.N. *Usp. Fiz. Nauk*, **147**, 6755 (1985).
13. Klimov V.V. *Nanoplasmonics* (Singapore: Pan Stanford, 2010; Moscow: Fizmatlit, 2009).
14. Nikolajeff F., Löfving B., Johansson M., et al. *Appl. Opt.*, **39**, 4842 (2000).
15. *Modern Electroplating*. Ed. by M.Schlesinger, M.Paunovic (New York: John Wiley & Sons, 2000) p.147.
16. Barmina E.V., Lau Truong S., Bozon-Verduraz F., Levi G., Simakin A.V., Shafeev G.A. *Kvantovaya Elektron.*, **40**, 346 (2010) [*Quantum. Electron.*, 4**0**, 346 (2010)].
17. Barmina E.V., Stratakis E., Fotakis C., Shafeev G.A. arXiv: 1003.2796v1 [cond-mat.mes-hall] (2010).
18. Bonse J., Munz M., Sturm H. *J. Appl. Phys.*, **97**, 013538 (2005).
19. Borowiec A., Haugen H.K. *Appl. Phys. Lett.*, **82**, 4462 (2003).
20. Golosov E.V., Ionin A.A., et al. *Phys. Rev. B*, **83**, 115426 (2011).
21. Soifer V.A. *Komp'yut. Opt.*, **32**, 110 (2008).
22. Golosov E.V., Ionin A.A., Kolobov Y.R., Kudryashov S.L., Ligachev A.E., Makarov S.V., Novoselov Y.N., Seleznev L.V., Sinitsyn D.V. *Appl. Phys. A,* DOI 10.1007/s 00339-011-6323-2.
23. Rytov S.M. *Zh. Eksp. Teor. Fiz.*, **29**, 605 (1955).
24. Gaylord T.K., Baird W.E., Moharam M.G. *Appl. Opt.*, **25**, 4562 (1986).
25. Ono Y., Kimura Y., Ohta Y., Nishida N. *Appl. Opt.*, **26**, 1142 (1987).
26. Grann E.B., Varga M.G., Pommet D.A. *J. Opt. Soc. Am. A,* **12**, 333 (1995).
27. http://www.microresist.de/products/ormocers/ormocomp_en.htm.